Procedia Manufacturing

Volume 5, 2016, Pages 1369–1381

44th Proceedings of the North American Manufacturing Research Institution of SME http://www.sme.org/namrc

# Tool Rake Face Temperature Distribution when Machining Ti6Al4V and Inconel 718

Jean Carlos Garcia-Gonzalez, Wilfredo Moscoso-Kingsley, and Viswanathan Madhavan*

*Wichita State University, Wichita, U.S.A.*

**Abstract**

This paper is concerned with experimentally obtained full field temperature distributions at the interface between chip and tool – the tool rake face – for the machining of Ti6Al4V and Inconel 718. As part of the work presented herein, temperature distributions at the chip-tool interface were obtained using a novel technique, near infrared thermography, which provides high accuracy for the target temperature range above 1250 K. During the study, transparent yttrium aluminum garnet (YAG) tools were used to provide an optical path to the chip-tool interface.

*Keywords:* Machining, Tool Temperature, Thermography, Titanium, Inconel

## 1 Introduction

This paper is concerned with experimentally obtained full field temperature distributions at the interface between chip and tool – the tool rake face – for the machining of Ti6Al4V and Inconel 718. As part of the work presented herein, temperature distributions at the chip-tool interface were obtained using a novel technique, near infrared thermography, which provides high accuracy for the target temperature range above 1250 K. During the study, transparent yttrium aluminum garnet (YAG) tools were used to provide an optical path to the chip-tool interface. The data should be useful in validation of finite element (FE) models for machining.

Attempts to measure temperature at the actual point where heat is generated in machining date back to the work of Shore (Shore, 1925) and Herbert (Herbert, 1926), who introduced the tool-work thermocouple technique. Among different methods that have been implemented since then stand out thermometry by the use of embedded thermocouples (Kitagawa, Kubo, & Maekawa, 1997), metallographic analysis (Wright & Trent, 1974; Smart & Trent, 1975) and radiometry, which in turn can be subdivided into pyrometry and infrared and near infrared thermography (Boothroyd, 1963; Jaspers, Dautzenberg, & Taminiau, 1998; Kus, Isik, Cemal Cakir, Coskun, & Özdemir, 2015; Lane,

*Corresponding Author. Mail to vis.madhavan@wichita.edu.

Selection and peer-review under responsibility of the Scientific Programme Committee of NAMRI/SME 

doi:10.1016/j.promfg.2016.08.107

Whitenton, Madhavan, & Donmez, 2013; Menon & Madhavan, 2014). The tool-work thermocouple technique is based on the existence of a thermoelectric effect at the chip-tool interface, provided that the workpiece and the tool materials are dissimilar. It can only measure the mean temperature at the chip-tool interface. While it is possible to place many thermocouples very close to the chip-tool interface (embedded thermocouples) to determine temperature distribution at this interface (Komanduri & Hou, 2001), the installation of these thermocouples can be cost intensive and extremely tedious. More importantly, multiple holes have to be drilled, which alters the heat conduction through the tool and reduces its strength. Metallographic techniques infer the chip-tool interface temperature from microstructural or hardness changes in the chip material directly in contact with the tool. Even though this method is capable of measuring temperature within ±25 K in the range of 900 K to 1150 K (Wright & Trent, 1974), it is only applicable to tool materials whose microstructural change is very sensible to temperature, such as high speed steels.

In thermography, the radiation emitted by different points of a hot source in the infrared or near infrared portion of the spectrum can be converted into source temperature using a power law in the form (Menon & Madhavan, 2014; Menon, 2013):

$$T = a\left(\frac{S}{\varepsilon\tau}\right)^{b}, \tag{1}$$

where $T$ is the temperature of a particular point on the object (in Kelvin, K), $S$ is a measure of the radiation intensity reaching the camera pixel where the object point is imaged, also known as the "counts" and expressed in arbitrary units, $\varepsilon$ is the emissivity of the object's surface (dimensionless), and $\tau$ is the camera exposure time (in milliseconds, ms). The constants in Equation 1 are obtained after calibration with a blackbody placed directly on top of the tool rake face. The calibration procedure is well described by Menon and Madhavan (Menon & Madhavan, 2014; Menon, 2013). If the radiation is measured with a high speed camera, thermography can return the temperature distribution of the source surface with high spatial and temporal resolution. This technique has been used to investigate the temperature distribution of the cutting tool (Miller, Mulholland, & Anderson, 2003; Narayanan, Krishnamurthy, Chandrasekar, Farris, & Madhavan, 2001), the workpiece (Boothroyd, 1963), the chip side faces (Sutter & Ranc, 2007), the top of the chip (Jaspers, Dautzenberg, & Taminiau, 1998), and the chip-tool interface (Davies, Yoon, Schmitz, Burns, & Kennedy, 2003). The use of thermography to determine the chip-tool interface temperature distribution requires optical access to the tool rake face. This has been accomplished through the use of tools that are transparent in the infrared and the near infrared.

Müller-Hummel and Lahres (Müller-Hummel & Lahres, 1994; Müller-Hummel & Lahres, 1995) and Müller-Hummel et al. (Müller-Hummel, Lahres, Mehlhose, & Lang, 1997) used tools furbished with a 5-µm thick layer of chemical vapor deposition (CVD) diamond, which had a 500-µm thick window on a portion of the tool rake face. The window was sufficiently strong to withstand the cutting forces. A mirror underneath the window projected an image of the radiation emitted by the chip surface in contact with the window during the three-dimensional (3D) cutting of titanium and aluminum alloys. The camera was sensible to infrared radiation. The aim of the work was to find a correlation between chip-tool interface temperature and tool wear. Temperatures as high as 2000 K were reported for Ti6Al4V at machining velocities of about 2.5 m/s and feeds of about 300 µm/rev; and for AlZnMgCu1.5, at 21.7 m/s machining velocity and 400 µm/rev feed, temperatures were as high as 800 K. According to work reported by Davies et al. (Davies, Yoon, Schmitz, Burns, & Kennedy, 2003), for the temperature range produced at the machining velocity and feed that were applied above, the uncertainty in emissivity in the infrared leads to a relatively large error in temperature estimate. That is, about +/- 50 K. In addition to the high uncertainty inherent to infrared thermography, the CVD diamond window allowed only partial observation of the temperature field at the tool rake face. More accurate methods for observation of the full field temperature distribution at the tool rake face are desirable.

Narayanan et al. (Narayanan, Krishnamurthy, Chandrasekar, Farris, & Madhavan, 2001) measured the temperature distribution of the chip-tool interface when cutting brass in a two-dimensional (2D)

orthogonal arrangement using optically transparent sapphire tools. These tools were optically transparent in both the infrared and near infrared bands, and thus allowed the use of multi-wavelength high speed infrared pyrometry. These sapphire tools were much simpler than the CVD tools of Müller-Hummel and Lahres, and the multi-wavelength technique compensated for unknown emissivity values. The results showed that the highest temperature occurred in the zone of metal deposits some distance away from the cutting edge and on sides of the chip-tool contact. Temperatures as high as ~700 K were reported at machining velocities of about 1.5 m/s and feeds of about 50 μm/rev. While sapphire is sufficiently transparent and inexpensive to allow full size tools to be made, due to its significant decrease in hardness above 1000 K, cutting tools made out of this material are not suitable for the Ti6Al4V and Inconel 718 materials targeted in this paper.

According to work by Menon and Madhavan (Menon & Madhavan, 2014; Menon, 2013), temperature measurements in near infrared thermography are less sensitive to uncertainty in emissivity than in infrared thermography. For near infrared thermography, a temperature of 1250 K is related to an uncertainty in temperature of less than 10 K. Moreover, the cutting tool material that was implemented in this work, yttrium aluminum garnet (YAG) crystals, are virtually transparent and extremely hard. The YAG crystals are also sufficiently inexpensive to allow full size tools to be made to facilitate full field tool rake face temperature observations. These are the reasons that made near infrared thermography and YAG tools the preferred choice for this paper.

# 2 Experimental

The machining experiments for the observation of tool temperature were carried out using a very rigid and high speed custom built lathe. The setup was arranged in a way that allowed the cutting tool to be held stationary while the rotating workpiece was fed into the tool, as shown in Figure 1. The loop stiffness of the lathe was in the order of 100 N/μm. The spindle was capable of rotating at up to 10,000 rpm. The workpieces were prepared from solid rods of either annealed Ti6Al4V or solution treated Inconel 718. The rods were all turned to 25.4 mm diameter (OD). Then, drilling and boring was completed to form tubes. The Ti6Al4V tubes had wall thickness = 1.07 mm, and the Inconel 718 tubes had wall thickness = 1.44 mm. The tubes were held by a collet on the lathe that allowed a firm installation with minimal runout. Since the rotating workpiece was a narrow wall tube, the machining configuration approximated 2-D orthogonal cutting. For Ti6Al4V, the emissivity was taken as 0.5, as per information gathered from prior work by Menon and Madhavan (Menon & Madhavan, 2014; Menon, 2013). For Inconel 718, the emissivity was taken as 0.33, as per information gathered from (Greene, Finfrock, & Irvine Jr, 2000; Raj & Prabhu, 2013).

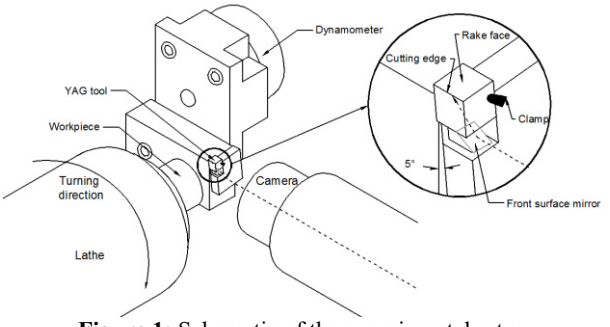


**Figure 1:** Schematic of the experimental setup.

The YAG tools, supplied by Red Optronics, were 6-mm cubes having 12 potentially usable cutting edges. To increase the toughness of the YAG cubes, they were subject to an annealing treatment in air

in a Sensor Tech Corp. STT-1600-2.75-12 high temperature tube furnace. The YAG cubes were heated at a rate of 4 °C per minute, held at 1600 °C for 10 hours, and then cooled back to ambient temperature at a rate of 4 °C per minute. Care was taken to observe the edge condition of these tools under the microscope after annealing and prior to cutting using a MicroXAM optical profilometer. The same profilometer was used to observe the tool condition after cutting. The edge radius, as received from Red Optronics, was about 2.5 µm. The YAG cubes were held by a specially designed tool holder that allowed cutting at -5° rake angle and +5° relief angle, as depicted in Figure 1. The fixture supported the cubes on three mutually orthogonal faces. A clamp secured the cubes in place. The tool holder had a small pocket under the cube support, where a 1.1-mm thick glass front-surface mirror was mounted. The mirror directed the radiation emitted by the surface of the chip in contact with the tool rake face towards the camera, as shown in Figure 1. The tool holder was mounted on a Kistler 9367B tri-axial dynamometer that measured the cutting and thrust forces.

The radiation was imaged by a LaVision Imager Intense cooled low noise camera that was mounted on a Leica MZ16 stereomicroscope. A 1x plan apochromatic objective (numerical aperture = NA = 0.14) and a 1.5x coupler were used along with an 8x optical zoom to achieve an effective magnification of 12x on the 1376 x 1024 charge-coupled device (CCD) array in the camera. Therefore, each 6.45-µm square pixel was equivalent to approximately a 0.56-µm square region of the tool surface, and the total field of view was 770 µm x 570 µm. Figure 2 shows a magnified view of the cutting arrangement from the point of view of the imaging system. The figure illustrates the orientation of the cutting edge, as observed by the camera. A direct image of the tool rake face is projected on the CCD array to the right of the cutting edge. The rake face also reflects from the flank face. This reflected image reaches the CCD array, and projects to the left of the cutting edge. Figure 3A shows an actual *in situ* image recorded by the camera, and Figure 3B shows the conversion to temperature vs. distance from the cutting edge superimposed on a micrograph of the tool rake face. To convert radiation intensity to temperature, Equation 1 was applied pixel-by-pixel. The constants *a* and *b* in Equation 1 were 1036.65 and 0.0647, respectively. These constants were defined through a blackbody calibration performed by Menon and Madhavan (Menon & Madhavan, 2014; Menon, 2013) just before the start of the experimental work presented herein.

The camera had a 12 bit dynamic range (4095 counts), with readout noise less than 2.5 counts, dark noise less than 1 count, nonlinearity less than 1%, and non-uniformity less than 0.6%. The laboratory was darkened to start the experiments. Background images at room temperature were taken prior to each cutting experiment, which usually resulted in intensity of about 40 counts. The background images were averaged and subtracted pixel-by-pixel from the *in situ* images.

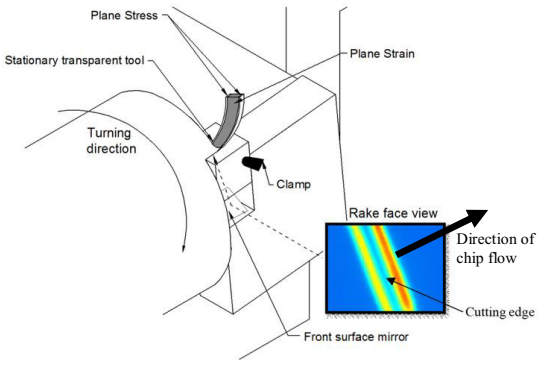


**Figure 2:** Magnified view of the cutting arrangement from the point of view of the camera.

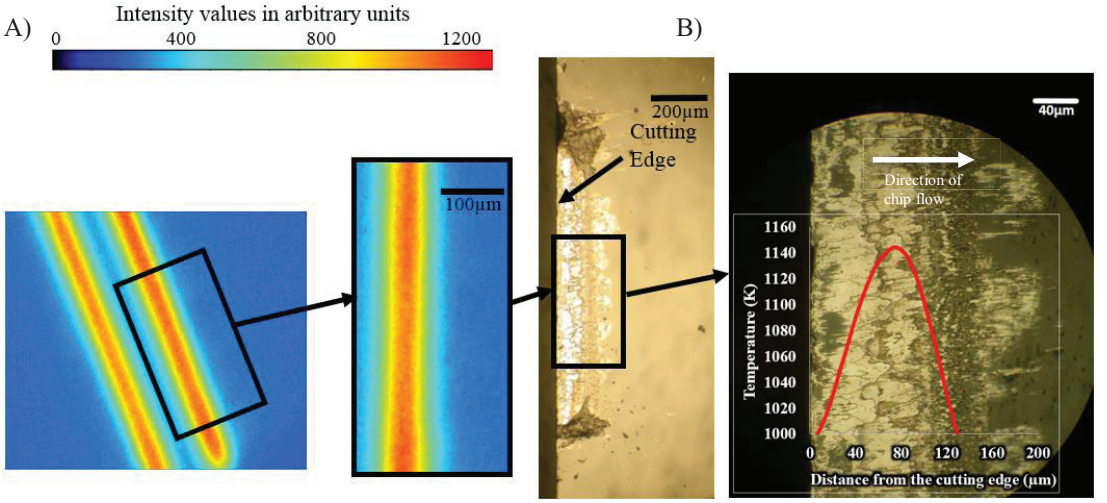


**Figure 3:** A) Actual image recorded by the camera system. B) Conversion to temperature vs. distance from the cutting edge superimposed on a micrograph of the tool rake face.

The camera control software allowed grouping several pixels into one – a technique known as "binning". For binning, 64 pixels on an 8 x 8 square sub-array were combined. This means that the 1376 x 1024 CCD array was converted into a 1376/8 x 1024/8 = 172 x 128 array. The grouping reduced the pixel readout time, and consequently, the scan rate was increased. For instance, when binning was used, more than 12 frames could be captured during a cutting experiment at machining velocity = 1 m/s. In contrast, when binning was not used, only 3 frames could be captured. The exposure time was selected on the basis of intensity reaching the CCD array. The exposure time must be limited to a sufficiently small value to avoid CCD array saturation (which occurs at > 4095 counts).

The acquisition of the sequence of images and the lathe feed were triggered by a digital signal. Therefore, image acquisition and lathe feed were started simultaneously. The lathe was pre-set at a fixed distance from the tool using precision-made plastic shims to prepare for cutting and, at the same time, prevent any damage to the cutting edge resulting from direct tool-workpiece contact prior to the cutting. Except for variations arising from uncertainty in workpiece positioning, each cut was set to 6 workpiece rotations, which means that the length of each cut was equal to $\pi$ x OD x 6 = $\pi$ x 25.4/1000 m x 6 = 0.48 m. After reaching the end of the cut, the feed was stopped, but the workpiece was retracted away from the tool after one extra rotation. This ensured that the workpiece surface was perpendicular to its axis of rotation, and produced a smooth initial rotation during the next cut. It is important to note that for each cut, a brand new tool (tool cutting edge) was utilized, and that this cutting edge only engaged with the workpiece during the six feeding rotations (plus the extra rotation without feed at the end of the cut.) Labview was used to record the machining forces as well as the trigger signal. After the cutting, the recorded machining forces and the trigger signal, as well as the acquired images were analyzed for timing accuracy, and to obtain force and temperature data. For both the Ti6Al4V and the Inconel 718 workpieces the following was performed. First, the feed ($f$) was kept constant at 50 µm/rev, while the machining velocity was set to 1, 2, 3 and 4 m/s. Then, the machining velocity ($V$) was kept constant at 1 m/s, while the feed was set to 25, 50, 75, 100 and 125 µm/rev.

# 3 Results

## 3.1 Experiments on Ti6Al4V

Figure 4 shows the temperature at the chip-tool interface as a function of distance from the cutting edge for machining velocities ranging from 1 m/s to 4 m/s, and a constant feed of 50 µm/rev. Figure 6 shows the temperature at the chip-tool interface as a function of distance from the cutting edge for feeds ranging from 25 µm/rev to 125 µm/rev, and a constant machining velocity of 1 m/s. Multiple temperature curves are shown which correspond to repetitions to obtain statistical significance. The curves were constructed as explained in the Experimental (Section 2), and represent the average temperature taken over a 200-µm wide portion of the total cut width, from the center of the chip-tool contact, as shown in Figure 3. Figure 5 shows the peak temperature as a function of machining velocity, and Figure 7 shows the peak temperature as a function of feed. These figures were constructed as follows: 1) For each repetition in Figure 4 or Figure 6, the maximum temperature is determined; 2) For a given machining velocity, the average and the standard deviation of the peak temperature are calculated using the corresponding maximum temperature values; 3) The average value is taken as a statistical measure of the peak temperature along the tool rake face and the standard deviation as the statistical error.

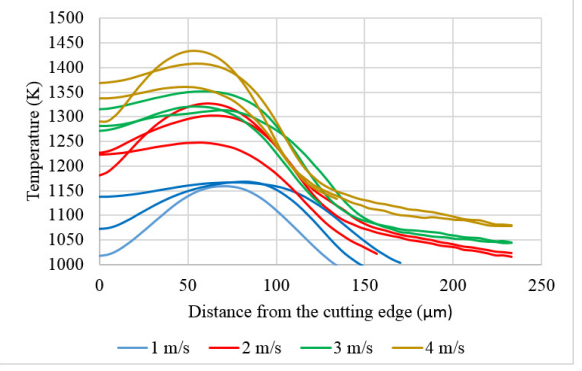


**Figure 4:** Tool temperature as a function of distance from the cutting edge, for several machining velocities. **Work material: Ti6Al4V**. Conditions: tool = YAG, tool rake angle = -5°, tool relief angle = 5°, feed = 50 µm/rev, cut width = 1.07 mm.

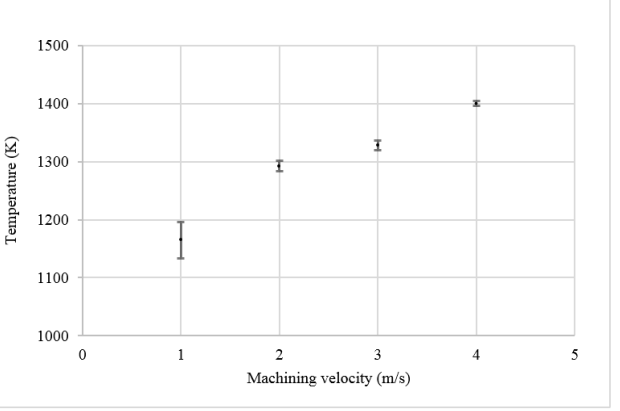


**Figure 5:** Peak tool temperature as a function of machining velocity. **Work material: Ti6Al4V**. Conditions: tool = YAG, tool rake angle = -5°, tool relief angle = 5°, feed = 50 µm/rev, cut width = 1.07 mm.

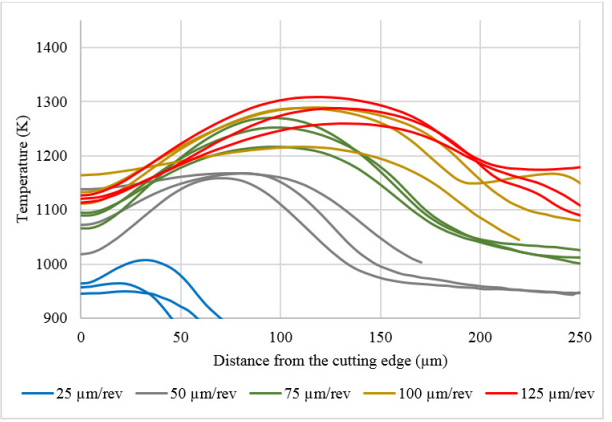


**Figure 6:** Tool temperature as a function of distance from the cutting edge, for several feed values. **Work material: Ti6Al4V**. Conditions: tool = YAG, tool rake angle = -5°, tool relief angle = 5°, machining velocity = 1 m/s, cut width = 1.07 mm.

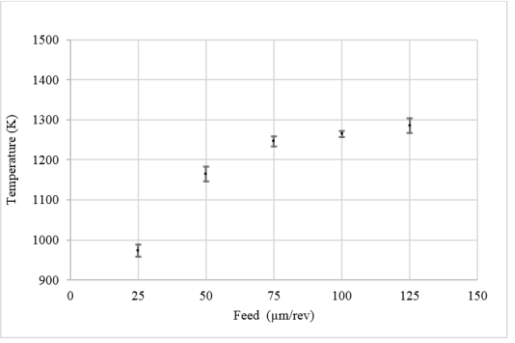


**Figure 7:** Peak tool temperature as a function of feed. **Work material: Ti6Al4V**. Conditions: tool = YAG, tool rake angle = -5°, tool relief angle = 5°, machining velocity = 1 m/s, cut width = 1.07 mm.

From the data in Figure 4 and the error bars in Figure 5, for a feed of 50 µm/rev and a given machining velocity, the resulting temperature curves are separated from each other no more than ~30 K near the location of the peak temperature, and no more than 50 to 100 K near the tool cutting edge. For the latter case, the lower error of ~50 K corresponds to lower machining velocities (1 and 2 m/s), and the higher error of ~100 K corresponds to the higher machining velocities (3 and 4 m/s). From the data in Figure 6 and the error bars in Figure 7, for a machining velocity of 1 m/s, the temperature near the location of the peak temperature is defined within ~30 K, and the temperature near the cutting edge is defined within ~50 K. As the machining velocity is increased from 1 m/s to 4 m/s, the temperature at the cutting edge also increases, whereas when the feed is increased from 50 µm/rev to 125 µm/rev, the temperature at the cutting edge does not change significantly. Only the reduced feed of 25 µm/rev produced a significantly lower temperature at the cutting edge.

Figure 8 shows the peak tool rake face temperature vs. machining power, and Figure 9 shows the peak tool temperature vs. friction power. To construct the plots, the machining power was taken as the product of the cutting force measured by the dynamometer and the machining velocity. The friction power (friction at the rake face) was taken as the product of the friction force measured by the dynamometer and the chip velocity. To estimate chip velocity, the machining velocity was multiplied by the cutting ratio (feed/chip thickness). The chip thickness was measured with a micrometer. These figures suggest that the peak temperature is related to both the machining and the friction power through a power law. This implies that the peak temperature is affected by machining power regardless of the source – velocity or feed – producing the power level.

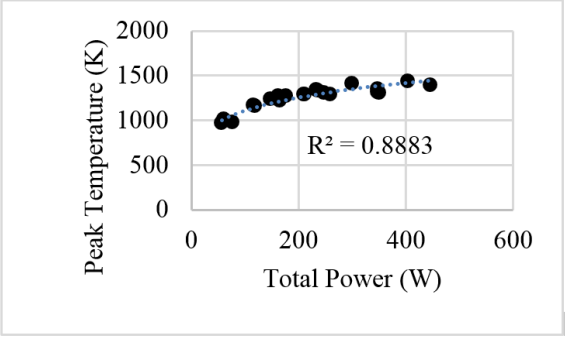


**Figure 8:** Peak temperature at the rake face vs. cutting power (total power). **Work material: Ti6Al4V**. Conditions: tool = YAG, tool rake angle = -5°, tool relief angle = 5°, cut width = 1.07 mm.

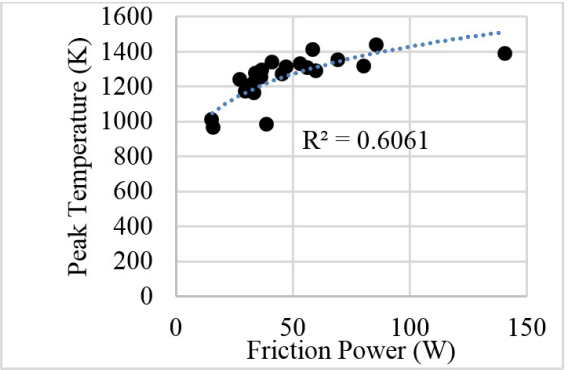


**Figure 9:** Peak temperature at the rake face vs. friction power. **Work material: Ti6Al4V**. Conditions: tool = YAG, tool rake angle = -5°, tool relief angle = 5°, cut width = 1.07 mm.

## 3.2 Experiments on Inconel 718

Figure 10 shows the temperature at the chip-tool interface as a function of distance from the cutting edge for machining velocities ranging from 1 m/s to 4 m/s, and a constant feed of 50 μm/rev. Figure 12 shows the temperature at the chip-tool interface as a function of distance from the cutting edge for feeds ranging from 25 μm/rev to 125 μm/rev, and a constant machining velocity of 1 m/s. Multiple temperature curves are shown which correspond to repetitions to obtain statistical significance. The curves were constructed as explained in the Experimental (Section 2), and represent the average temperature taken over a 200-μm wide portion of the total cut width, from the center of the chip-tool contact, as shown in Figure 3. Figure 11 shows the peak temperature as a function of machining velocity, and Figure 13 shows the peak temperature as a function of feed. These figures were constructed as follows: 1) For each repetition in Figure 10 or Figure 12, the maximum temperature is determined; 2) For a given machining velocity, the average and the standard deviation of the peak temperature are calculated using the corresponding maximum temperature values; 3) The average value is taken as a statistical measure of the peak temperature along the tool rake face and the standard deviation as the statistical error.

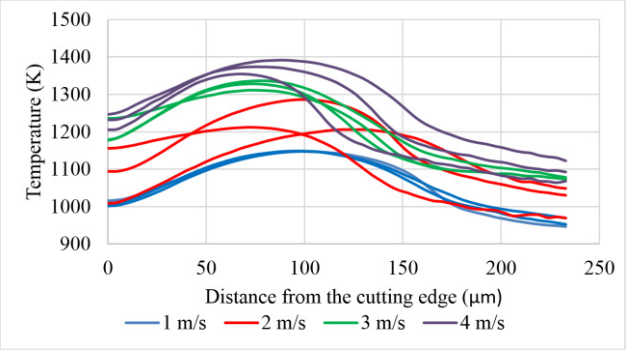


**Figure 10:** Tool temperature as a function of distance from the cutting edge, for several machining velocities. **Material: Inconel 718**. Conditions: tool = YAG, tool rake angle = -5°, tool relief angle = 5°, feed = 50 µm/rev, cut width = 1.44 mm.

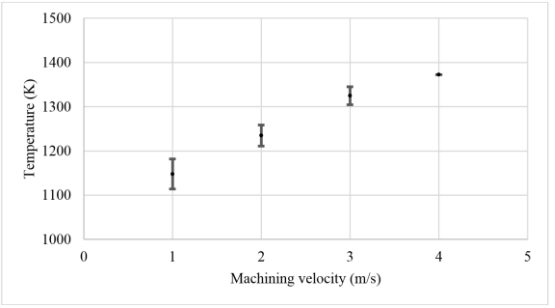


**Figure 11:** Peak tool temperature as a function of machining velocity. **Material: Inconel 718**. Conditions: tool = YAG, tool rake angle = -5°, tool relief angle = 5°, feed = 50 µm/rev, cut width = 1.44 mm.

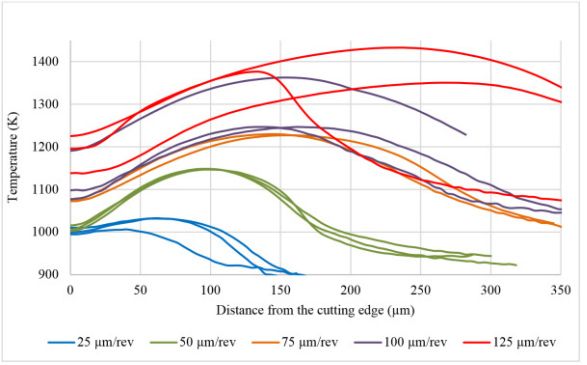


**Figure 12:** Tool temperature as a function of distance from the cutting edge, for several feed values. **Material: Inconel 718**. Conditions: tool = YAG, tool rake angle = -5°, tool relief angle = 5°, machining velocity = 1 m/s, cut width = 1.44 mm.

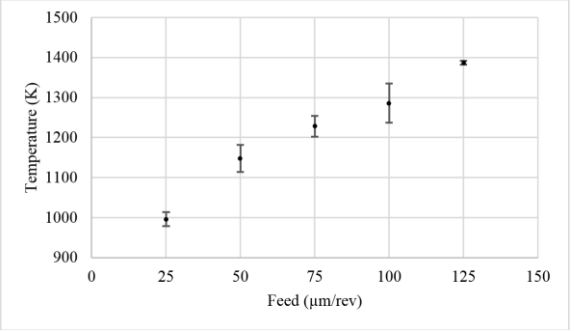


**Figure 13:** Peak tool temperature as a function of feed. **Material: Inconel 718**. Conditions: tool = YAG, tool rake angle = -5°, tool relief angle = 5°, machining velocity = 1 m/s, cut width = 1.44 mm.

From the data in Figure 10 and Figure 12, and the error bars in Figure 11 and Figure 13, it is clear that the temperature profiles show considerable scatter. While there is a peak temperature some distance from the cutting edge, and increasing machining velocity and feed produce an increase in temperature, repeating a given cutting condition can result in temperature curves that are separated from each other ~100 K. The odd consistency seems to be at random, occurring at both low or high machining velocity and small or large feed. As the machining velocity is increased from 1 m/s to 4 m/s, or the feed is increased from 25 μm/rev to 125 μm/rev, the temperature at every point along the chip-tool contact also increases.

Figure 14 shows the peak tool rake face temperature vs. machining power, and Figure 15 shows the peak tool temperature vs. friction power. To construct the plots, the machining power was taken as the product of the cutting force measured by the dynamometer and the machining velocity. The friction power (friction at the rake face) was taken as the product of the friction force measured by the dynamometer and the chip velocity. To estimate chip velocity, the machining velocity was multiplied by the cutting ratio (feed/chip thickness). The chip thickness was measured with a micrometer. These figures suggest that the peak temperature is related to both the machining and the friction power through a power law. This implies that the peak temperature is affected by machining power regardless of the source – velocity or feed – producing the power level.

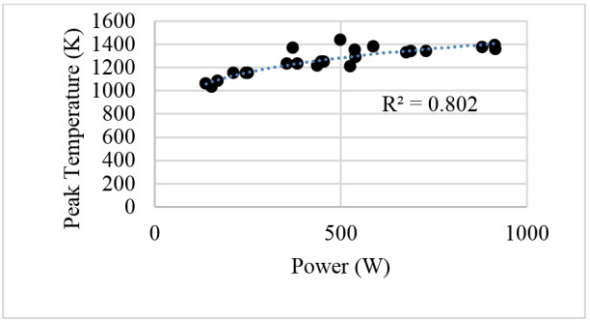


**Figure 14:** Peak temperature at the rake face vs. cutting power (total power). **Work material: Inconel 718**. Conditions: tool = YAG, tool rake angle = -5°, tool relief angle = 5°, cut width = 1.44 mm.

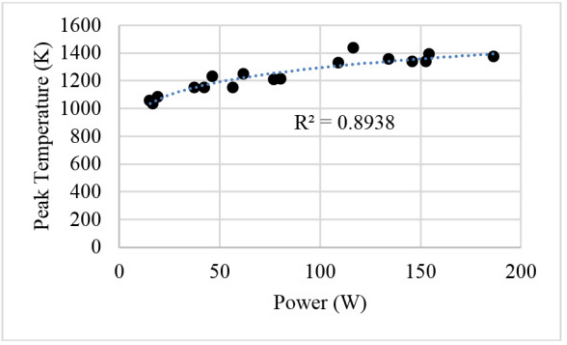


**Figure 15:** Peak temperature at the rake face vs. friction power. **Work material: Inconel 718**. Conditions: tool = YAG, tool rake angle = -5°, tool relief angle = 5°, cut width = 1.44 mm.

# 4 Discussion

An inspection of Figure 4 to Figure 7 and Figure 10 to Figure 13 reveals that the peak temperature associated with the Ti6Al4V and the Inconel 718 workpieces, for the same machining velocity/feed condition, are the same to within tens of degrees Kelvin. The only exception seems to be for machining velocity = 1 m/s at the high feeds. The peak temperature in Ti6Al4V shows a plateau at ~1250 K, for feeds from 75 to 125 µm/rev. This plateau is not defined in Inconel 718, where at the highest feed of 125 µm/rev the peak temperature reaches the maximum value of ~1400 K.

Other similarities between Ti6Al4V and Inconel 718, in terms of temperature at the chip-tool interface, can be observed. The peak temperature gets closer to the tool cutting edge as the machining velocity increases (Figure 4 and Figure 10), while as the feed increases, the peak temperature gets farther away from the cutting edge (Figure 6 and Figure 12). It is interesting to note that the peak temperature is always a finite distance away from the cutting edge. For both Ti6Al4V and Inconel 718, based on Figure 4, Figure 6, Figure 10, and Figure 12; and the print left by the chip on the tool rake face (e.g., Figure 3), this distance is about 1 to 1.5 times the feed; and it is always between the cutting edge and the point where the chip departs from the tool. This fact is consistent with a total temperature field that is being produced by both plastic work at the primary shear plane and additional plastic work arising from the frictional interaction between chip and tool. The frictional heating accumulates with distance from the cutting edge, and the contribution to temperature rise from it increases monotonically with distance from the cutting edge. The heat from the primary shear plane diffuses more quickly to points along the rake face that are closer to the cutting edge. The effect is the creation of a temperature profile that first rises with distance from the cutting edge and then drops.

As a final note, the peak temperature seems strongly correlated to total machining power and friction power (friction power at the rake face). If the power increases, either due to an increase in machining velocity or an increase in feed, the peak temperature also increases. The effect on peak temperature from an increase in machining velocity seems to be the same as that from an increase in feed. This suggests the existence of a dimensionless quantity related to machining conditions and tool-work material properties that controls peak temperature.

The temperature measurements performed herein are from a relatively low speed imaging system capable of ~10 frames per second. It is known that both titanium alloys and Inconel form pronounced shear bands. However, the shear bands occur at frequencies that are in the order of 1 KHz. Shear banding has a direct effect on shear strain, so it should have a direct effect on temperature. The measurement of such temperature variations will require a high speed imaging system. This will be the focus of future research.

# 5 Conclusions

Other parameters being equal, when a YAG tool is used, the chip-tool interface temperature when cutting Ti6Al4V and Inconel 718 are about the same, except at large feeds of more than 100 µm. These temperatures are in the order of 1000 K. The distance from the cutting edge to the peak temperature decreases with an increase in machining velocity, and increases with an increase in feed. The peak temperature occurs at a finite distance from the cutting edge that is smaller than the length of the chip-tool contact zone. Machining power and/or friction power at the tool rake face seem to have direct control over the peak temperature at the chip-tool interface.

# Acknowledgements

This work was supported by the Engineering Expansion Grant given to the state of Kansas to Wichita State University.

# References

Boothroyd, G. (1963). Temperatures in Orthogonal Metal Cutting. *Proceedings of the Institution of Mechanical Engineers, 177*(29), 789-810.

Davies, M. A., Yoon, H., Schmitz, T. L., Burns, T. J., & Kennedy, M. D. (2003). Calibrated Thermal Microscopy of the Tool-Chip Interface in Machining. *Machining Science and Technology, 7*(2), 167-190. doi:10.1081/MST-120022776

Greene, G. A., Finfrock, C. C., & Irvine Jr, T. F. (2000). Total hemispherical emissivity of oxidized Inconel 718 in the temperature range 300-1000°C. *Experimental Thermal and Fluid Science, 22*, 145-153.

Herbert, E. (1926). The Measurement of Cutting Temperatures. *Proceedings of the Institution of Mechanical Engineers, 110*, 289-329.

Jaspers, S., Dautzenberg, J., & Taminiau, D. (1998). Temperature Measurement in Orthogonal Metal Cutting. *The International Journal of Advance Manufacturing Technology, 14*, 7-12.

Kitagawa, T., Kubo, A., & Maekawa, K. (1997). Temperature and Wear of cutting tools in high-speed machining of Inconel 718 and Ti-6Al-6V-2Sn. *Wear, 202*, 142-148.

Komanduri, R., & Hou, Z. B. (2001). A review of the experimental technique for the measurement of heat and temperatures generated in some manufacturing processes and tribology. *Tribology International, 34*, 653-682.

Kus, A., Isik, Y., Cemal Cakir, M., Coskun, S., & Özdemir, K. (2015). Thermocouple and Infrared Sensor-Based Measurement of Temperature Distribution in Metal Cuttin. *Sensors, 15*, 1274-1291. doi:10.3390/s150101274

Lane, B., Whitenton, E., Madhavan, V., & Donmez, A. (2013). Uncertainty of Temperature Measurements by Infrared Thermography for Metal Cutting Applications. *Metrologia, 50*(6), 637-653.

Menon, T. (2013). Full-field infrared thermography at tool-chip interface through transparent cutting tool while machining TI-6AL-4V.

Menon, T., & Madhavan, V. (2014). Infrared Thermography of the Chip-Tool Interface through Transparent Cutting Tools. *Proceedings of NAMRI/SME, 42*.

Menon, T., & Madhavan, V. (2014). Infrared Thermography of the Chip-Tool Interface through Transparent Cutting Tools. *Proceedings of NAMRI/SME, 42*.

Miller, M. R., Mulholland, G., & Anderson, C. (2003). Experimental Cutting Tool Temperature Distributions. *Journal of Manufacturing Science and Engineering, 125*, 667673. doi:10.1115/1.1621425

Müller-Hummel, P., & Lahres, M. (1994). Infrared temperature measurement on diamond coated tools during machining. *Diamond and Related Materials, 3*(4-6), 765-769.

Müller-Hummel, P., & Lahres, M. (1995). Quantitative measurement of temperatures on diamond-coated tools during machining. *Diamond and Related Materials, 4*, 1216-1221.

Müller-Hummel, P., Lahres, M., Mehlhose, J., & Lang, G. (1997). Measurement of temperature on diamond-coated tools during machining processes. *Diamond Films and Technology, 7*(4), 219-232.

Narayanan, V., Krishnamurthy, K., Chandrasekar, S., Farris, T. N., & Madhavan, V. (2001). Measurement of the Temperature Field at the Tool-Chip Interface in Machining. *Proceedings of 2001 ASME International Mechanical Engineering Congress and Exposition.* New York, NY.

Raj, V. C., & Prabhu, S. V. (2013). Measurement of surface temperature and emissivity of different materials by two-colour pyrometry. *Review of Scientific Instruments, 84*(12), 124903.

Shore, H. (1925). Thermoelectric measurement of cutting tool temperatures. *Journal of the Washington Academy of Sciences, 15*(5), 85-88.

Smart, E. F., & Trent, E. M. (1975). Temperature distribution in tools used for cutting iron, titanium and nickel. *INT. J. PROD. RES., 13*(3), 265-290.

Sutter, G., & Ranc, N. (2007). Temperature fields ina chip during high-speed orthogonal cutting - An experimental investigation. *International Journal of Machine Tools & Manufacture, 47*, 1507-1517.

Wright, P. K., & Trent, E. M. (1974). Metallurgical appraisal of wear mechanisms and processes on high-speed-steel cutting tools. *Metals Technology*, 13-23.